THE ASTROPHYSICAL JOURNAL, 538:233–240, 2000 July 20

THE FORMATION OF A MULTIPLE PLANETARY NEBULA: *HUBBLE SPACE TELESCOPE*/WFPC2 OBSERVATIONS OF KjPn 8

J. A. LÓPEZ,[1] J. MEABURN,[2] L. F. RODRÍGUEZ,[3] R. VÁZQUEZ,[1] W. STEFFEN,[4] AND M. BRYCE[2]
Received 1999 December 1; accepted 2000 February 23

ABSTRACT

KjPn 8 is an extreme polypolar planetary nebula with a large-scale structure characterized by a giant biconical envelope. Spasmodic bipolar ejections in changing directions have occurred over thousands of years to create this peculiar nebula. Narrowband images of the core of KjPn 8 have now been obtained with the Wide Field Planetary Camera 2 on board the *Hubble Space Telescope* (*HST*) and are reported here. The central star is finally revealed in these observations, and its compact nebular core is resolved into a remarkably young elliptical ring, currently expanding at only 16 km s^{-1}. This ring is the ionized inner region of larger molecular CO and H_2 counterparts, all sharing the same orientation. The highest speed and youngest outflows are perpendicular to this central ring, which is identified as the latest event in the creation of this nebula. It is shown that the formation history of KjPn 8 has involved two distinct and consecutive planetary nebulae-like events, probably originating from a binary core evolution with components of very similar mass. These characteristics indicate that KjPn 8 may be a rare object in our Galaxy and the first ever detected of this class.

Subject headings: ISM: jets and outflows — planetary nebulae: individual (KjPn 8) — radio lines: ISM

1. INTRODUCTION

In recent times the *Hubble Space Telescope* (*HST*) has resolved many planetary nebulae (PNs) with peculiar characteristics that mainly reveal a diversity of point-symmetric structures and multiple, collimated outflow directions (for a recent compilation of *HST* images of PNs, see Terzian & Hajian 2000). Although these types of phenomena had been confirmed to exist from ground-based observations in a handful of objects since the early 1990s (cf. Miranda & Solf 1992; López, Meaburn, & Palmer 1993; Schwarz 1993), the database now provided by the *HST* clearly indicates the need for a reformulation of current theories to explain the origin and evolution of PNs; this is a current major challenge in PN research. However, as it is shown in this paper, even among this wealth of new data KjPn 8 represents a singularly unusual case.

Appreciation of the extraordinary nature of the polypolar planetary nebula KjPn 8 has unfolded during a series of ground-based observations (López, Vázquez, & Rodríguez 1995; López et al. 1997, 1999; Huggins et al. 1997; Steffen & López 1998; Vázquez, Kingsburgh, & López 1998; Forveille et al. 1998). The recognition of distinct outflows along different axes in KjPn 8 led originally to their interpretation as the action of a bipolar rotating episodic jet, or BRET (López et al. 1995). Similar BRET-type phenomena have been recognized in many other planetary nebulae (e.g., López 1997; Sahai & Trauger 1998; Guerrero 2000). In the BRET interpretation, it is assumed that the symmetry axis of a bipolar collimated outflow rotates (or precesses) and episodic ejections along it create a distinct S-shaped, point-symmetric configuration or polypolar structures. Fairly contiguous events or smooth transitions in the variations of direction of the outflow are usually implied by the morphologies observed. In contrast to the known cases, in KjPn 8 the notoriously different position angles between its bipolar flows indicate the occurrence of abrupt changes in outflow directions and substantial differences in times between ejection events.

Recently, a central molecular disk has been revealed in maps of emissions from CO (see Forveille et al. 1998) and H_2 (López et al. 1999). The optical structure of the core had not been resolved from ground-based observations, but subarcsecond $\lambda = 6$ cm MERLIN observations suggested the possible presence of a star with a high mass-loss rate near the center of the molecular disk (López et al. 1999). It has required optical imagery with the *Hubble Space Telescope*, presented here, to reveal the inner, elliptical ionized ring that constitutes the nebular core of KjPn 8. Furthermore, in these optical observations the central star has been imaged for the first time and is found to be at the center of this ionized central ring, though not coinciding with the MERLIN source. In addition, the first measurement of the ring's expansion velocity has been obtained. In this paper, the data collected over several years and passbands on KjPn 8 are analyzed and discussed in relation to these latest *HST* and ground-based observations.

2. OBSERVATIONS AND RESULTS

The Wide Field Planetary Camera 2 (WFPC2) images were obtained through filters F673N, F658N, and F656N centered on the [S II] $\lambda\lambda$6716, 6731, [N II] λ6584, and Hα nebular emission lines; independent images with integration times between 400 and 500 s each were obtained through each filter for total integration times of 3000, 2000, and 2800 s, respectively. The passband (FWHM) and peak transmission efficiency for the [S II], [N II], and Hα filters are $\Delta\lambda = 47.2$ Å, $T = 87\%$; $\Delta\lambda = 28.5$ Å, $T = 79.7\%$; and $\Delta\lambda = 21.4$ Å, $T = 77.9\%$, respectively. The observing strategy involved a linear dithering procedure which aids in removing cosmic rays and improved the image quality of the WF2 camera, on which the core was centered, by combining subpixel dithered images (Mutchler & Fruchter 1997). The data arrays were drizzled with a 0.5 pixel fraction

[1] Postal address: Instituto de Astronomía, UNAM-Ensenada, Apdo. Postal 877, Ensenada, B.C. 22800, México.
[2] Jodrell Bank Observatory, University of Manchester, Macclesfield, Cheshire SK11 9DL, England.
[3] Instituto de Astronomía, UNAM-CU, Apdo. Postal 70-264, D.F. 04510, México.
[4] Instituto de Astronomía y Meteorología, Universidad de Guadalajara, Av. Vallarta 2602, Guadalajara, Jalisco 44130, México.

resulting in pixel dimensions of 0.05×0.05 arcsec^2 in the final images.

An absolute coordinate grid for the core region of KjPn 8 had been derived previously (López et al. 1999) from a SuperCOSMOS scan of a POSS-I Schmidt plate. The astrometric fit for this grid has been found to have an absolute accuracy of $\pm 0''.4$. An improved coordinate grid with an absolute accuracy of $\pm 0''.13$ has now been obtained from observations with the Carlsberg Meridian Telescope (CMT) of four field stars within $\pm 2'$ of the core of KjPn 8. The data in this paper are now referred to these Carlsberg coordinates.

In addition, new deep (1800 s) long-slit spectral observations of the core of KjPn 8 have been obtained at higher spectral resolution than those available previously (López et al. 1997) in subarcsecond seeing conditions. The Manchester echelle spectrometer (MES) (Meaburn et al. 1984) was combined with the f/7.9 focus of the 2.1 m San Pedro Mártir UNAM telescope (1999 September 7). This spectrometer has no cross-dispersion. A filter of 90 Å bandwidth was used to isolate the 87th order containing the Hα and [N II] λ6584 nebular emission lines. A single-slit 70 μm wide $\equiv$ 6 km s^{-1} and $0''.9$ was used on this occasion. A Tektronix CCD with 1024×1024, 24 μm, square pixels was the detector ($\equiv 0''.3$ pixel^{-1} along the slit and a 0.05 Å pixel^{-1} along the dispersion axis). Seeing conditions were $\sim 0''.8$–$0''.9$ during these observations. The spectra were calibrated to ± 0.5 km s^{-1} accuracy against that of a Th/Ar arc lamp. The slit was placed right across the nebular core of KjPn 8 with orientation north-south.

3. DISCUSSION

3.1. *Structural Components and Dynamical Times*

It is the $14' \times 4'$ extent of the largest lobes (P.A. $\approx 72°$) with knots C_1-C_2 at their extremities as shown in Figure 1*a* compared with the few arcsecond diameter of the bright nebular core that first indicated the unusual nature of this nebula. Also, secondary smaller lobes, delineated by knots A_1-A_2 (P.A. $\approx 126°$) in Figure 1*a*, have a distinctly different axis from C_1-C_2. A third pair of symmetric knots, labeled B_1-B_2 in earlier papers (cf. López et al. 1995), are no longer considered to represent an independent ejection axis. Their location in high-density rings of the large envelope (see Steffen & López 1998) indicate their likely origin as a consequence of the outburst that produced the A_1-A_2 high-velocity outflows as the effects of the shock waves are spread over the neighboring regions.

Steffen & López estimate an age of $\sim 9 \times 10^3$ yr for the giant envelope using a distance of 1 kpc to KjPn 8 in their hydrodynamic model. Here we adopt the distance of 1.6 kpc derived by Meaburn (1997) on firmer grounds. Thus, the largest lobes, C_1-C_2, from their linear dimensions and kinematics (López et al. 1997) must be (1–2) $\times 10^4$ yr old and still consistent with the Steffen & López model within their range of parameters. The knots A_1-A_2 aligned with the axis of the ring revealed at the core of KjPn 8 by the *HST* (see Figs. 1*b* and 1*c*) have a kinematical age $\leq$3400 yr as given directly by their angular displacements from the nebular core combined with measurements of their expansion proper motions (Meaburn 1997). This particular timescale estimation is independent of the distance to KjPn 8.

Images of the elliptically shaped, $5''.2 \times 2''.7$ ring around the central star, observed with the *HST*/WFPC2 camera in the [S II] $\lambda\lambda$6716, 6731, [N II] λ6584, and Hα nebular emission lines are shown in Figure 2. This ring is clearly the ionized inside surface of a 7″ diameter ring of excited H_2 (see Fig. 3), itself located within a central 30″ diameter massive CO disk (Forveille et al. 1998). The location and approximate dimensions of this CO disk are indicated in Figure 1*b*. The CO disk thickens considerably farther from the central star to form the central walls of the bipolar cavities that culminate in the high-speed knots A_1-A_2. The axis of this central ionized ring, similar to those of its molecular counterparts, is along P.A. 126° and closely aligned with an axis through knots A_1-A_2. In Figure 1*c*, the ionized filaments nearest the core seem to delineate the outer walls of the molecular disk.

The ionized ring, if circular, must also have its P.A. 126° axis tilted at $\approx 59°$ with respect to the sight line to produce the ring's elliptical appearance in the *HST* images. This tilt angle is satisfyingly similar to the 53° tilt of the common outflow axis of the knots A_1 and A_2 as deduced from their kinematics (López et al. 1997; Meaburn 1997) with A_2 tilted away from the observer. Significantly, confidence in the distance estimation to KjPn 8 of 1600 $\pm$ 230 pc, deduced by a combination of proper motion and kinematical measurements (Meaburn 1997), is bolstered by this angular similarity. A linear scale for KjPn 8 of 7.76×10^{-3} pc arcsec^{-1} can therefore be safely adopted to permit estimations of the kinematical ages of the various features of KjPn 8.

The ionized ring itself, if expanding at a constant 16 km s^{-1} (see Fig. 4), would only take $\sim 1.25 \times 10^3$ yr to reach its present $2''.7$ ($\equiv$0.02 pc) radius. However, this kinematic age is likely an overestimate for the core has probably just reached photoionization conditions in a more recent past (see below). These temporal differences indicate that the A_1-A_2 high-velocity ($\sim \pm 320$ km s^{-1}) knots and associated bipolar outflows were formed prior to the present central ionized ring. Furthermore, the largest features, culminating in the knots C_1-C_2, must have formed along a different ejection axis well before any of the central ionized and molecular circumstellar structures were created.

3.2. *The A_1-A_2 Jets*

Jets in planetary nebulae seem to be formed predominantly during the preplanetary nebula stage, and their lifetime should only be a few thousand years at most (e.g., Reyes-Ruiz & López 1999), for the mass-loss rates involved at this stage need to be high. The bipolar lobes leading to A_1 and A_2 do not seem highly collimated at present, nor have signs of highly collimated material along A_1-A_2 been detected in the *HST* images emerging from the nebular core. The A_1 and A_2 bow shocks travel at highly supersonic velocities, and the outflow velocity of the associated material leading to them is observed to decrease toward the core (López et al. 1997). Therefore, it is probably reasonable to identify the origin of the A_1-A_2 high-speed knots as ballistic jets that are currently mainly momentum-driven flows; i.e., the conditions for collimation and jet generation are no longer operative.

There is a prominent filament protruding in projection directly north from the core (see Fig. 1*c*) that has been intersected by the slit and shows an expanding cone of faint material (see Fig. 4) opening northward. The filament seems to be one of the ionized edges of the structure that forms the northwest lobe leading to A_2. The blueshifted, brighter section of this expanding feature reaches an expanding

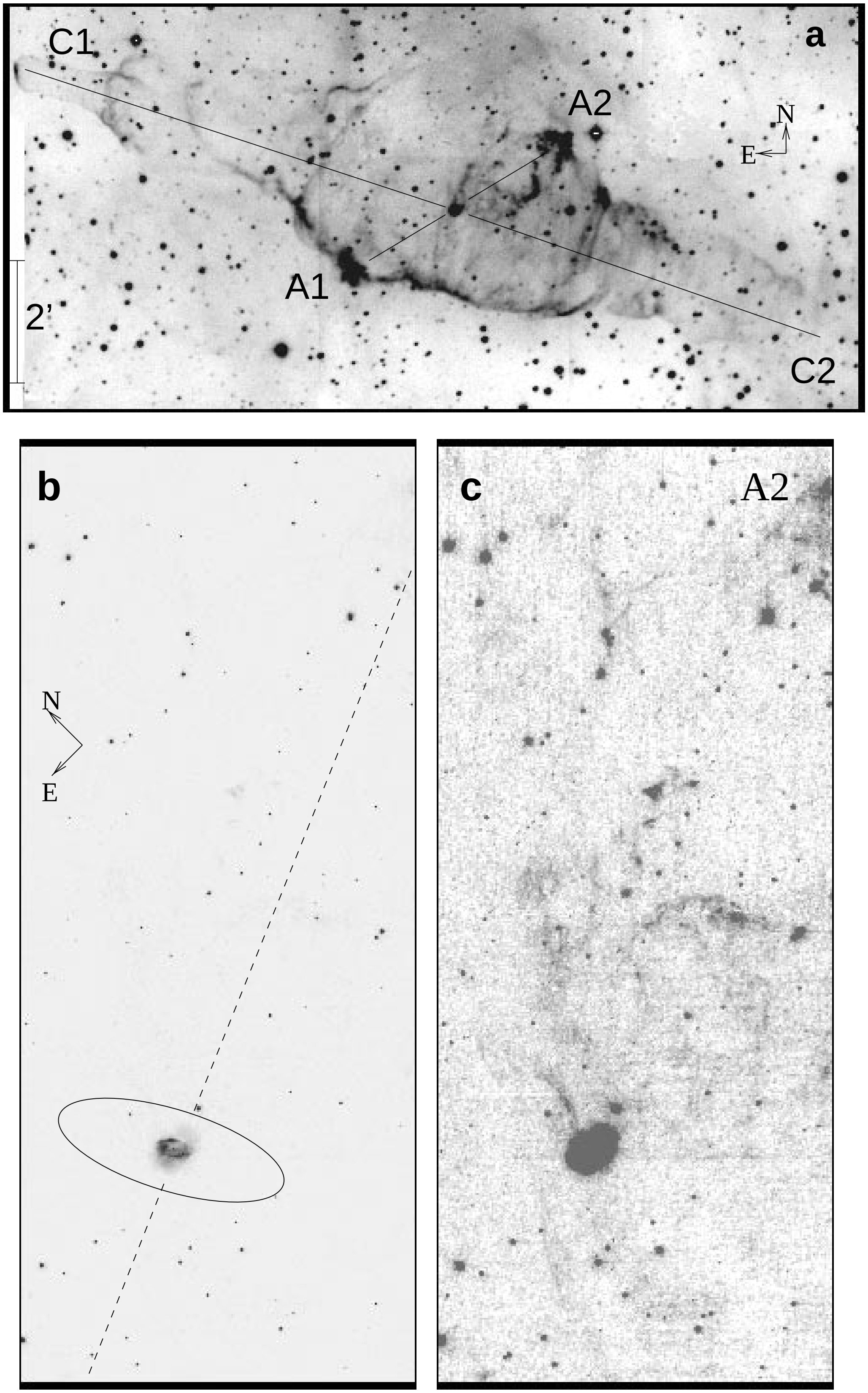

FIG. 1.—Panel *a* shows a deep Hα wide-field, ground-based image of the polypolar nebula KjPn 8. The symmetric knots C_1-C_2 (P.A. 72°) and A_1-A_2 (P.A. 126°) are located at the tips of independent bipolar outflows. The whole nebula is $14' \times 4'$ in extent. Both bottom panels contain the same region covered by the WF2 + WF3 CCDs of the WFPC2 camera, shown at different gray scales to highlight different features. In panel *b* the ring structure and orientation of the compact nebular core with respect to the A_2-A_1 bipolar outflows is appreciated; this is to be compared with panel *c*, where the filamentary structure leading to the A_2 bow shock can be seen. The ellipse drawn around the core in panel *b* indicates the location and approximate dimensions of the massive CO disk found by Huggins et al. (1997). The spatial resolution of the image in panel *c* has been slightly degraded in order to enhance the nebular features. Note that the orientation of the bottom panels, indicated in panel *b*, differ from that of the top panel.

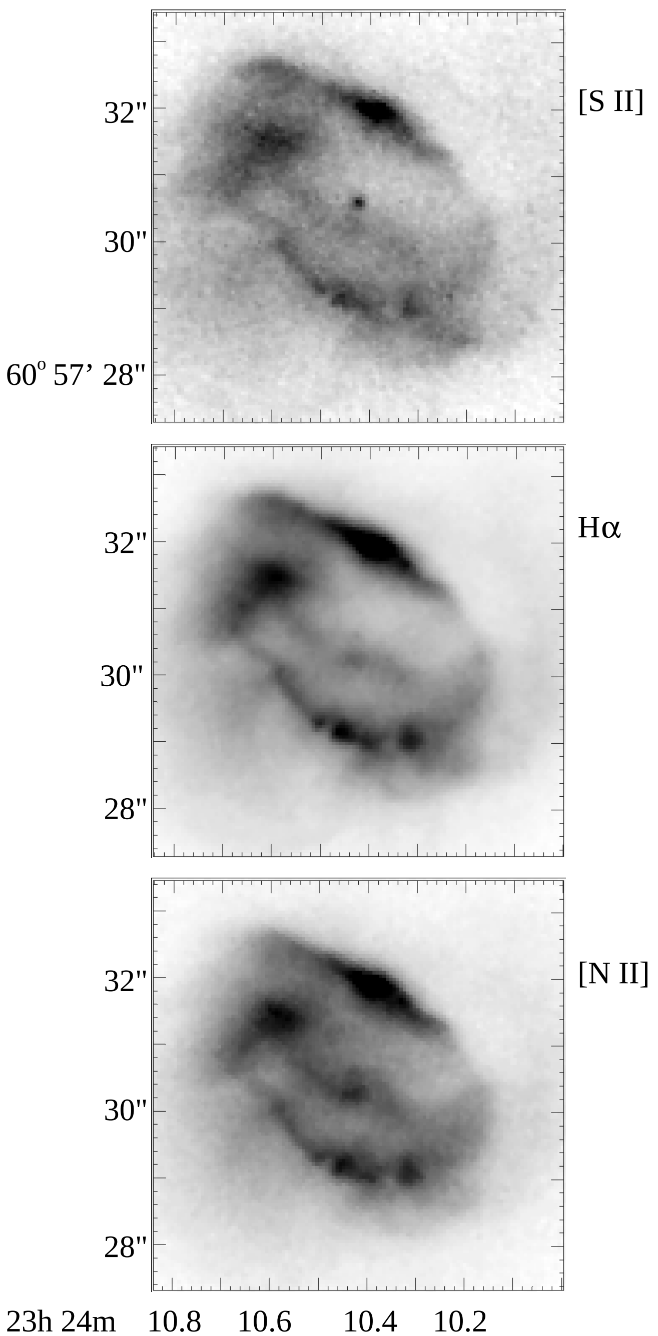

FIG. 2.—Images of the annular nebula located at the geometric center of KjPn 8 (see Figs. 1*a* and 1*b*), obtained with the WFPC2 camera on board the *HST*. The final drizzled data arrays have resulting pixel dimensions of 0.05×0.05 arcsec^2. The core contains a star right at the center of the tilted ionized ring and is clearly detected in the [S II] image, which has the widest passband and longest integration time of all. Coordinates are J2000 and have been derived from CMT observations with an accuracy of 0.″13.

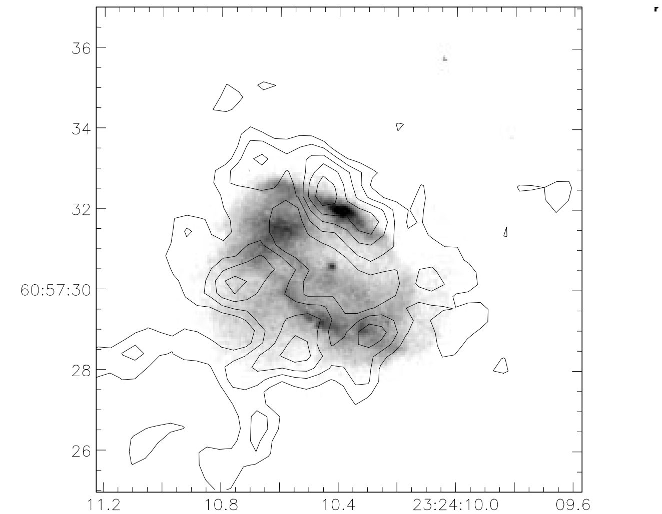

FIG. 3.—Contour map of the H_2 $v = 1 \rightarrow 0$ $S(1)$ (2.122 μm) emission of the core of KjPn 8 is shown overlaid on the [S II] *HST* image of the core of KjPn 8 where the central star is apparent. The H_2 emission surrounds and shares the morphology and orientation of the ionized ring, as also does a larger CO disk (see Fig. 1*b*) confirming a second heavy mass-loss episode in KjPn 8. Coordinates are J2000 and as in Fig. 2.

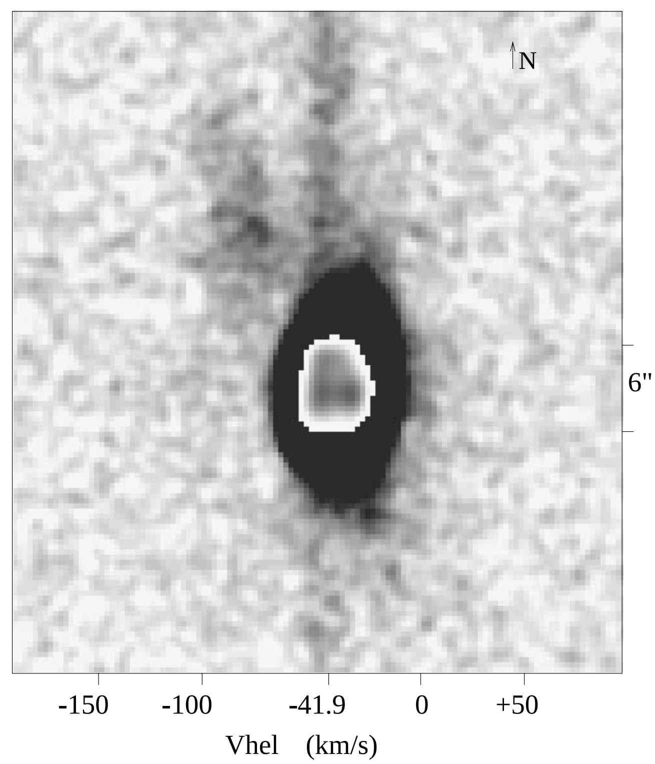

FIG. 4.—Negative gray-scale representation of the [N II] λ6584 position-velocity array for the core of KjPn 8. The slit is oriented north-south, and north is indicated in the figure. A Gaussian filter has been applied to enhance faint features, such as the expanding "cone" of emission to the north of the core where the more intense, blueshifted component is seen to reach $V_{\rm hel} \approx -100$ km s^{-1}. The bright inner core region, superposed on the figure, shows line splitting corresponding to the expansion of the ring, which has been resolved for the first time with the narrow slit used in the present observations and amounts to 16 km s^{-1}, considering the ring's tilt. The more extended nebular material surrounding the core expands at $\approx$40 km s^{-1}, as found previously by López et al. (1997).

velocity of ≈ -60 km s^{-1} with respect to the systemic velocity. These kinematic data, together with those contained in the east-west slits in López et al. (1997), probe the presence of current outflowing material from the core but not as a jetlike outflow anymore. The kinematic data indicate that the A_1-A_2 jet system must have indeed formed during the preplanetary nebula stage of the present nebular core that has developed the ionized ring and was actively (energy) driven for only a short time.

3.3. *Physical Characteristics of the Nebular Core*

The Hα flux from the nebular core, contained within a 4″.5 diameter aperture, has been derived from the *HST* images following the prescription by Dudziak & Walsh (1997) that takes into account the known flux contribution leaking from the [N II] λ6584 emission line into the N656 WFPC2 Hα filter. The *HST* images yield $F_{\mathrm{H}\alpha} = 2.4 \times 10^{-13}$ ergs s^{-1} cm^{-2}, which compares favorably with the wide-slit spectroscopic flux obtained by Vázquez et al. (1998) ($F_{\mathrm{H}\alpha} = 1.9 \times 10^{-13}$ ergs s^{-1} cm^{-2}). Also, the Hα flux predicted by the 3.5 cm VLA continuum observations, $S_{(3.5\ \mathrm{cm})} = 0.77$ mJy (López et al. 1995), compares reasonably well with the dereddened *HST* Hα flux considering that a certain amount of internal extinction is likely to be present in this case. Using $c_{\mathrm{H}\beta} = 0.71$ (Vázquez et al. 1998), $F_{\mathrm{H}\alpha} = 7.4 \times 10^{-13}$ ergs s^{-1} cm^{-2}, whereas, as $S_{(3.5\ \mathrm{cm})}$ mJy $= 9.47 \times 10^{11} F_{\mathrm{H}\alpha}$, $F_{\mathrm{H}\alpha} = 8.1 \times 10^{-13}$ ergs s^{-1} cm^{-2} is predicted if the radio emission has a thermal origin.

In KjPn 8, the ratio of molecular to ionized mass derived by Huggins et al. (1997) and Forveille et al. (1998) is large, $M_m/M_i \gtrsim 60$, with $M_m \gtrsim 0.03\ M_\odot$ and $M_i \approx 5 \times 10^{-4}\ M_\odot$. Since the optical nebula is expected to grow at the expense of the molecular material and considering the small dimensions of the central ionized ring and its low-excitation nebular spectrum (López et al. 1995), the physical characteristics of the core of KjPn 8 are representative of a very young PN. Moreover, its ionic abundances (Vázquez et al. 1998), with enhanced He and N, correspond to extreme type I PNs that are identified with massive progenitors, having masses in excess of 2.4 $M_\odot$ (Peimbert & Torres-Peimbert 1983) which should evolve quickly during the early PN stage toward higher effective temperatures and consequently higher excitation conditions. This implies that the core of KjPn 8 has only reached photoionization conditions during the last few hundred years and again indicates that the formation of the bipolar high-speed (A_1-A_2) outflows occurred shortly before, during the preplanetary nebula stage. These arguments strengthen the conclusion that the formation of the giant bipolar envelope had its origin in a different event, unrelated to the creation of the present nebular core and associated high-velocity, bipolar outflows.

3.4. *The Giant Biconical Envelope*

The origin of extended, low surface brightness structures or halos in planetary nebulae precede the formation of the main nebular shell and originate in the thermally pulsating asymptotic giant branch (AGB) phase (e.g., Vassiliadis & Wood 1994). It would thus be tempting to suggest that the giant bipolar structure of KjPn 8 had a similar origin. There are, however, noticeable differences in terms of both morphology and kinematics that argue against this possible analogy. Halos are produced by isotropic mass-loss processes and thus are mostly spherical. Even in some cases where clear signs of early bipolar development are apparent, the underlying halo is seen to be composed of concentric circular structures (e.g., Sahai et al. 1998; Kwok, Su, & Hrivnak 1998). Most halos are kinematically inert or have very low expansion velocities (e.g., Bryce et al. 1992; Meaburn et al. 1991; Hajian et al. 1997), typically less than 10 km s^{-1}. In KjPn 8, the giant axisymmetric structure has a lateral expansion velocity across its axis of 40 km s^{-1} and more than 100 km s^{-1} along it. Furthermore, in order to reproduce these characteristics together with its peculiar "biconical" shape, the envelope has been convincingly modeled as the result of the action of an episodic, collimated, bipolar outflow impinging on the surrounding environment (Steffen & López 1998). Therefore, if any (spherical or ellipsoidal) halo was formed, this must have preceded the formation of the giant bipolar envelope and the collimated outflows that shaped it. The halo plus ambient material were blown by these first bipolar jets (the precursors that led to the formation of C_1-C_2) which have now ceased their activity. For the current core conditions, the associated CO and H_2 molecular material must be related to a second heavy mass-loss episode prior to the formation of the ionized nebular core. The disklike structure and common orientations of the molecular material and ionized nebular ring confirm their connection in this second event. These characteristics are incompatible with the expected conditions that the core must have had at the time when the C_1-C_2 bipolar outflows where triggered.

3.5. *The Stellar Core*

The characteristics of the central star are unknown. Its location, at 23$^{\mathrm{h}}$24$^{\mathrm{m}}$10$^{\mathrm{s}}$.408 and +60°57′30″.61, has been revealed for the first time in the present narrowband *HST*/WFPC2 observations shown here. Given the apparent rejuvenation process that the core has undergone, a "born-again" phenomenon (e.g., Iben 1995) may have occurred, similar to those inferred for hydrogen-deficient PNs (e.g., Harrington 1996; Peña et al. 1994), where a late thermal flash takes the PN back to near AGB conditions. However, the nebular core of KjPn 8 does not seem to be hydrogen deficient. Moreover, although high ionic abundances of He, N, O, and Ne have been found (Vázquez et al. 1998), these enhancements do not match the exotic values observed in born-again objects; they rather indicate an extreme type I PN from a massive progenitor. Furthermore, it seems unlikely that a born-again scenario alone could explain the other puzzling characteristics mentioned above, such as the direct association with massive molecular material and changes in orientation of the symmetry axes.

A MERLIN threshold detection of a point source at $\lambda = 6$ cm near the center of the ring was reported earlier by López et al. (1999). This emission was suggested as probably originating from the dense wind of the central mass-losing star, then yet undetected. However, the location of the central star, now revealed by the *HST* observations, does not coincide with the MERLIN source. Within the improved coordinate grid recently obtained with the CMT observations, the MERLIN source, at 23$^{\mathrm{h}}$24$^{\mathrm{m}}$10$^{\mathrm{s}}$.399 and +60°57′30″.14, closely coincides with the central emission maximum of the VLA-A $\lambda = 6$ cm map (see Fig. 5) and with a relatively bright nebular knot located 0″.34 (≈500 AU) south from the central star (see Fig. 6). The spatial coincidence of the MERLIN source and VLA-A maximum with this nebular knot indicates that a possible companion could be embedded here. Moreover, the panels in Figure 6 show the central 2 arcsec^2 of the core in the different filters; here it can be appreciated how the central star, clearly present in the [S II] filter, tends to vanish in the [N II] and Hα images, yet the nebular knot south of the star remains prominent at these wavelengths. The appearance of the central star in these images must be due to a combination of exposure times and filter characteristics (see § 2) with the spectral energy distribution of the star, which is unknown but assumed to be characteristic of a white dwarf or a PN nucleus. In addition, the spectral contribution from

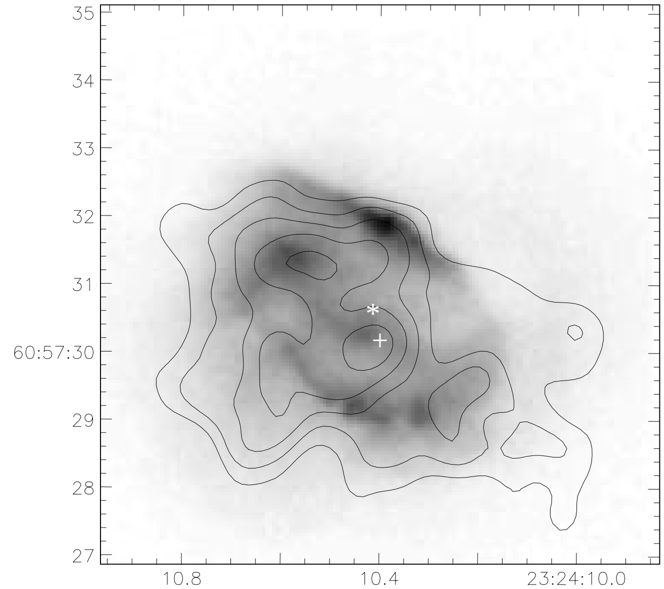

FIG. 5.—A 6 cm VLA-A contour map is shown overlaid on the Hα *HST* image of the core. The asterisk marks the position of the star detected by the *HST* and the cross the possible MERLIN point source, shown here to be coincident with the VLA-A maximum and the nebular knot located 0″.34 south of the central star. The linear VLA-A 6 cm contour intervals are evenly spaced between 30 and 110 μJy. The half-power beamwidth of the VLA observations is 0″.9.

a very close companion, at a separation $\lesssim$100 AU, would not be resolved in these observations, and its possible presence cannot be ruled out. In that case, the spectral contribution from a possible close companion to the central star would be more easily revealed in the wider [S II] filter that may transmit some photospheric continuum emission.

The Hα flux contained in the nebular knot has been derived from the *HST* images. For a 0″.3 diameter aperture centered on the knot, the observed flux contained in this region corresponds to $F_{\mathrm{H}\alpha} = 6.72 \times 10^{-15}$ ergs s^{-1} cm^{-2}, which when dereddened becomes 2.03×10^{-14} ergs s^{-1} cm^{-2}. This is to be compared with the corresponding measured flux at $\lambda = 6$ cm, $S_{6\,\mathrm{cm}} = 70$ μJy, detected by MERLIN. Assuming an average electron temperature $T_e = 10^4$ K and the ionic abundance of He/H = 0.229 derived by Vázquez et al. (1998), $S_{6\,\mathrm{cm}}(\mathrm{Jy}) = 1.22 \times 10^9 F_{\mathrm{H}\alpha}$, then $F_{\mathrm{H}\alpha} = 5.75 \times 10^{-14}$ ergs s^{-1} cm^{-2} would be expected if the MERLIN radio source had a thermal origin. This comparison indicates that the emitting Hα flux from this region seems to be insufficient, by over a factor of 2, to account for the $\lambda = 6$ cm MERLIN emission. Possible explanations are the presence of substantial internal optical extinction or a nonthermal radio component to the MERLIN source.

4. THE FORMATION HISTORY OF KjPn 8

From the discussion in the previous sections, the general picture indicates the occurrence of two independent PN-like events, where the first of these forms the large biconical nebula at P.A. 72° and some (1–2) × 10^4 yr later a second event is responsible for the formation of the current young nebular core and associated high-speed bipolar outflows, at P.A. 126°. As discussed in the previous section, there are indications that the core may be binary, either with an unresolved close companion, at a separation of

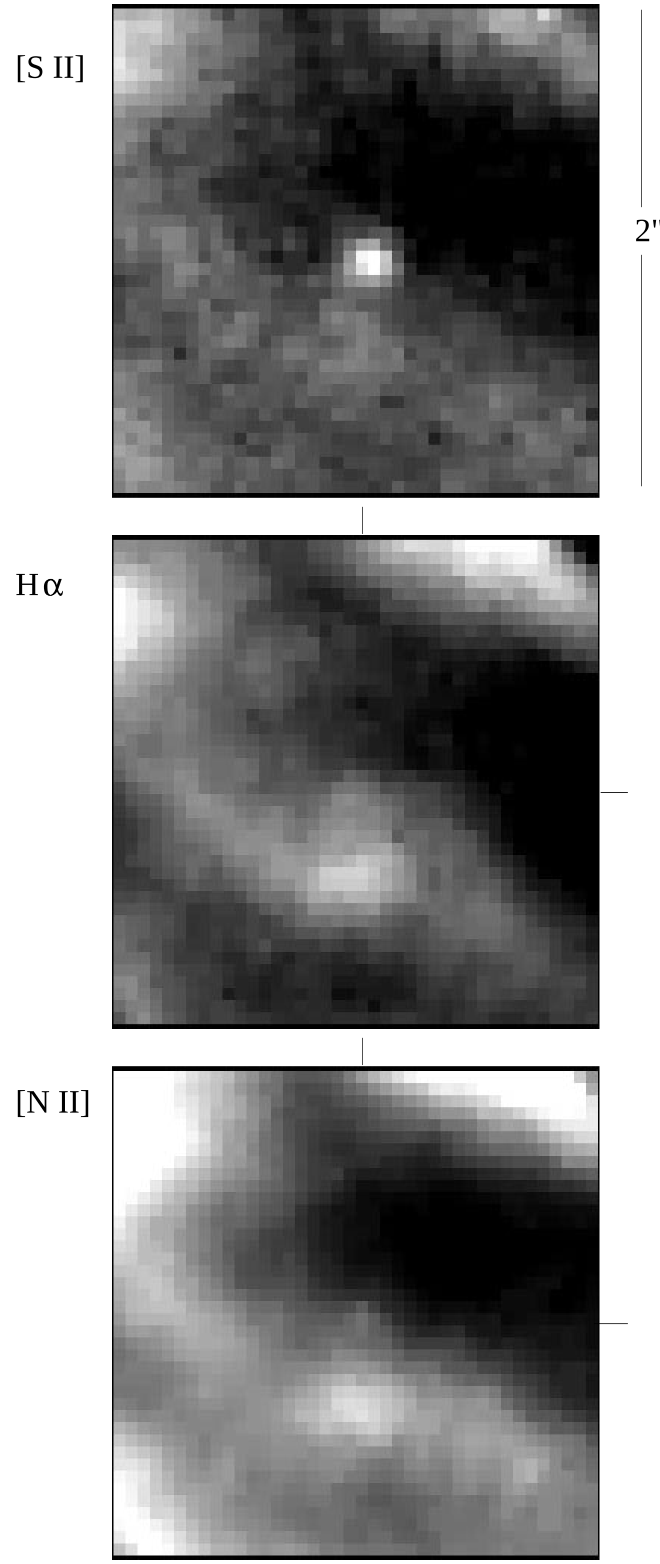

FIG. 6.—Enlargements of the central 2 arcsec^2 of the images in Fig. 2. The central star, clearly visible in the [S II] image, becomes much fainter, nearly disappearing, in the [N II] and Hα images; tick marks on the margins point to its location in these frames. However, a bright nebular knot located 0″.34 ($\approx$500 AU) south of the central star remains prominent, suggesting the presence of a bluer companion.

$\lesssim$100 AU, or a companion embedded in a nebular knot at $\sim$500 AU (or possibly both). The overall analysis leads now to consider alternatives of binary core evolution to understand the history of this extraordinary nebula. The possible paths in this context depend on the characteristics of the pair of stars and are diverse (e.g., Yungelson, Tutukov, & Livio 1993; Han, Podsiadlowski, & Eggleton 1995), but from the timescales involved in the processes the possible alternative can be restricted. For example, symbiotic nuclei, as those observed in some PNs and nova-like objects, are formed by a white dwarf plus a main-sequence or red giant star. If the white dwarf is the post-AGB progenitor of the large biconical nebula, then for the secondary to reach the PN stage it would take 10^7–10^9 yr, depending on its mass, and this path is ruled out.

Thus, the possible alternative is that we are witnessing the near simultaneous death of two relatively massive stars in a binary system either with a separation large enough for no effective mass transfer to take place (separations from several tens to a few hundred AU) or detached binaries (with separations of the order of a few tens of AU), where the evolution of an originally less massive secondary may be speeded up by wind accretion from the primary so both reach the PN stage one shortly after the other. A component in a binary core first evolving as a PN, if relatively massive, would be by now, $\approx 10^4$ yr later, a white dwarf of low luminosity, and a deep, blue broadband image would be needed for it to be detected.

Estimating the probability of having a binary system with very similar intermediate-mass components is quite uncertain. Assuming that for the intermediate-mass stars (the progenitors of type I PNs) the occurrence ratio of binaries to single stars is similar to the ratio of about 2:1 observed in F–G types in the solar neighborhood, and adopting a mass formation rate (Miller & Scalo 1979), we estimate that about 20 binaries with intermediate-mass members are formed per century in the Galaxy. Since the observable duration of PNs is of the order of 10^4 yr, we expect to find $\sim$2000 PNs having as progenitor one of the stars in a binary system of intermediate-mass objects. In addition, existing models for the formation of binary nuclei of PNs (e.g., Yungelson et al. 1993) predict a rate of 2–8 binary nuclei per century containing a CO or ONe dwarf plus a white dwarf as components. However, what are the probabilities that both stars are so similar as to end their lives within 10^4 yr of each other (the time separation between the creation of the extended and compact structures in KjPn 8)? The most massive of the stars that end as PNs have lifetimes of the order of 10^8 yr. Then, the possibility that in a binary system they coincide in reaching the last stages of their life within 10^4 yr is of the order of 10^{-4}. This probability would decrease in direct proportion to the stellar masses involved. According to the mass of the components, considering a range of 3–10 $M_\odot$, for a 10^4 yr time overlap to take place, the mass of the components would have to be coincident within 10^{-5} to 10^{-4}. Although the possibilities of this happening are low, they are not negligible. For example, there are indications that components in binary systems with periods below 100 yr show a tendency to have mass ratios close to 1 (Abt & Levy 1976). Furthermore, mass transfer may work toward making the masses similar.

5. CONCLUSIONS

The present *HST* observations have revealed the ionized core of a very young planetary nebula within an older bipolar nebula. Molecular gas is distinctly associated with the young core. In addition, recurrent conditions for bipolar jet formation with drastic variations in orientation of the symmetry axis of the outflows and conflicting timescales among the different components constitute the conundrum of this object.

The *HST* images provide indications of binarity in the core and the nebular ionic abundances are characteristic of massive progenitors; however, from the present data a more detailed history of the formation process cannot yet be discerned. We visualize two basic possibilities for the evolution of the putative binary core that may have originated the current structure of KjPn 8. (1) No effective mass transfer takes place among the binary components (separations of a few hundred AU) and each component evolves independently, one shortly after the other, to reach the PN stage. Bipolarity may develop in this case via magnetized winds as described in the MHD models by García-Segura et al. (1999), where the bipolar axes are defined by the rotation axis of each star. Another possibility is a common envelope process in each star with their own orbiting Jovian planets or brown dwarf–type companions that may lead via Roche lobe overflow to the formation of accretion disks (e.g., Reyes-Ruiz & López 1999) and the production of collimated outflows whose axes are also defined independently by each star. (2) A semidetached system (separations of a few tens of AU) where mass transfer operates by a wind accretion process (e.g., Mastrodemos & Morris 1999) may help to speed up the evolution of a less massive secondary. A novel approach to explain the development of bipolarity in these systems has been recently presented by Soker & Rappaport (2000), and it is interesting to note that in their model they predict the formation of a slowly expanding, dense, equatorial ring, as observed in the nebular core of KjPn 8, and bipolar outflows with a very narrow waist, as the lobe that leads to the A_2 knot. The opposite lobe is less well defined but by symmetry presumed to have similar characteristics. In this case, however, it is not clear how to explain the different orientations of the independent bipolar outflows (C_1-C_2 and A_1-A_2) since they would be expected to be defined by the same orbital plane in both cases. There are, however, some cases, e.g., in symbiotic binaries, where the outflows seem not to be orthogonal to the orbital plane (e.g., Mikolajewska 1999); also, in young objects the so-called phenomenon of quadrupolar outflows (e.g., Anglada, Rodríguez, & Torrelles 1996) seems to point to the possibility of producing two jets systems not necessarily aligned. These examples leave open the possibility for an unknown mechanism that may produce bipolar outflows from interacting binary systems whose axes do not remain normal to the orbital plane (rotation or precession effects do not apply in this particular case). A combination of both scenarios described above remains also a possibility, and only additional deep broadband *HST* images will help to reveal the stellar composition within the core of KjPn 8 and its likely path of evolution.

In summary, the data show that two PN-type events have been consecutively formed, producing bipolar outflows on each occasion and for each event having defined its own symmetry axis. The evolution of a binary core with components of very similar mass seems to be the interpretation best supported by the overall peculiar characteristics of KjPn 8. Of course, if many other similar systems are found in the Galaxy, an alternative explanation will be needed. However, if this is the correct explanation KjPn 8 may be a rare object in the Galaxy. So far, the indications are that KjPn 8 is indeed a very peculiar object.

J. A. L. thanks the WFPC2 team for their efficient support in reducing the dithered data. J. A. L. and L. F. R. acknowledge DGAPA-UNAM and CONACyT, México, for continuous financial support. We are grateful to Dafydd Wyn Evans for obtaining the CMT positions of field stars to permit accurate radio/optical comparisons. J. M. thanks the Royal Society for a grant to visit Mexico when part of this paper was written.

REFERENCES

Abt, H. A., & Levy, S. G. 1976, ApJS, 30, 273
Anglada, G., Rodríguez, L. F., & Torrelles, J. M. 1996, ApJ, 473, L123
Bryce, M., Meaburn, J., Walsh, J., & Clegg, R. E. S. 1992, MNRAS, 254, 477
Dudziak, G., & Walsh, J. R. 1997, in 1997 *HST* Calibration Workshop, ed. S. Casertano, R. Jedrzejewski, T. Keyes, & M. Stevens (Baltimore: STScI), 338
Forveille, T., Huggins, P. J., Bachiller, R., & Cox, P. 1998, ApJ, 495, L111
García-Segura, G., Langer, N., Rozyczca, M., & Franco, J. 1999, ApJ, 517, 767
Guerrero, M. 2000, in ASP Conf. Ser. 199, Asymmetrical Planetary Nebulae II: From Origins to Microstructures, ed. J. H. Kastner, N. Soker, & S. A. Rappaport (San Francisco: ASP), in press
Hajian, A. R., Frank, A., Balick, B., & Terzian, Y. 1997, ApJ, 477, 226
Han, Z., Podsiadlowski, P., & Eggleton, P. P. 1995, MNRAS, 272, 800
Harrington, J. P. 1996, in ASP Conf. Ser. 96, Hydrogen-deficient Stars, ed. C. S. Jeffery & U. Heber (San Francisco: ASP), 193
Huggins, P. J., Bachiller, R., Cox, P., & Forveille, T. 1997, ApJ, 483, L57
Iben, I. 1995, Phys. Rep., 250, 2
Kwok, S., Su, K. Y. L., & Hrivnak, B. J. 1998, ApJ, 501, L117
López, J. A. 1997, in IAU Symp. 180, Planetary Nebulae, ed. H. J. Habing & H. J. G. L. M. Lamers (Dordrecht: Kluwer), 197
López, J. A., Meaburn, J., Bryce, M., & Rodríguez, L. F. 1997, ApJ, 475, 705
López, J. A., Meaburn, J., Kuhn, O., Rodríguez, L. F., Muxlow, T. W. B., Pedlar, A., & Thomasson, P. 1999, ApJ, 518, 778
López, J. A., Meaburn, J., & Palmer, J. A. 1993, ApJ, 415, L135
López, J. A., Vázquez, R., & Rodríguez, L. F. 1995, ApJ, 455, L63
Mastrodemos, N., & Morris, M. 1999, ApJ, 523, 357
Meaburn, J. 1997, MNRAS, 292, L11
Meaburn, J., Blundell, B., Carling, R., Gregory, D. E., Keir, D. F., & Wynne, C. G. 1984, MNRAS, 210, 463
Meaburn, J., Nicholson, R., Bryce, M., Dyson, J., & Walsh, J. R. 1991, MNRAS, 252, 535
Mikolajewska, J. 1999, in ASP Conf. Ser. 188, Optical and Infrared Spectroscopy of Circumstellar Matter, ed. E. W. Guenther, B. Stecklum, & S. Klose (San Francisco: ASP), 291
Miller, G. E., & Scalo, J. M. 1979, ApJS, 41, 513
Miranda, L. F., & Solf, J. 1992, A&A, 260, 397
Mutchler, M., & Fruchter, A. 1997, in 1997 *HST* Calibration Workshop, ed. S. Casertano, R. Jedrzejewski, T. Keyes, & M. Stevens (Baltimore: STScI), 355
Peimbert, M., & Torres-Peimbert, S. 1983, in IAU Symp. 103, Planetary Nebulae, ed. D. R. Flower (Dordrecht: Reidel), 233
Peña, M., Torres-Peimbert, S., Peimbert, M., Ruiz, M. T., & Maza, J. 1994, ApJ, 428, L9
Reyes-Ruiz, M., & López, J. A. 1999, ApJ, 524, 952
Sahai, R., et al. 1998, ApJ, 492, L163
Sahai, R., & Trauger, J. T. 1998, AJ, 116, 1357
Schwarz, H. E. 1993, in Proc. Second ESO/CTIO Workshop, Mass Loss on the AGB and Beyond, ed. H. E. Schwarz (Garching: ESO), 223
Soker, N., & Rappaport, S. 2000, ApJ, 538, in press (preprint astro-ph/9911140)
Steffen, W., & López, J. A. 1998, ApJ, 508, 696
Terzian, Y., & Hajian, A. 2000, in ASP Conf. Ser. 199, Asymmetrical Planetary Nebulae II: From Origins to Microstructures, ed. J. H. Kastner, N. Soker, & S. A. Rappaport (San Francisco: ASP), in press
Vassiliadis, E., & Wood, P. R. 1994, ApJS, 92, 125
Vázquez, R., Kingsburgh, R., & López, J. A. 1998, MNRAS, 296, 564
Yungelson, L. R., Tutukov, A. V., & Livio, M. 1993, ApJ, 418, 794